American Mineralogist, Volume 92, pages 640–647, 2007

The system Ag-Au-Se: Phase relations below 405 K and determination of standard thermodynamic properties of selenides by solid-state galvanic cell technique

Evgeniy G. Osadchii* and Ekaterina A. Echmaeva

Institute of Experimental Mineralogy, Russian Academy of Sciences, Chernogolovka, Moscow District, 142432, Russia

Abstract

The existence of the only ternary compound, Ag_3AuSe_2 (fischesserite), in the Ag-Au-Se system was confirmed by solid-state annealing method. The selenium analog of petrovskaite (AgAuS) was not observed under the experimental conditions (in the temperature range of 350–773 K and own vapor pressure).

The solid-state reactions

$2Ag(cr) + Se(s) = Ag_2Se(cr)$
$Ag(cr) + Ag_3AuSe_2(cr) = 2Ag_2Se(cr) + Au(cr)$
$3Ag(cr) + 2AuSe(s) = Ag_3AuSe_2(cr) + Au(cr)$

were studied by the electromotive force (EMF) technique in all solid-state galvanic cells with Ag_4RbI_5 as a solid electrolyte. The experiments were run in a dry argon gas flow at atmospheric pressure.

The following standard thermodynamic properties of the stable phases were determined at 298.15 K and 1 bar (10^5 Pa):

$\Delta_f G°(Ag_2Se$, low naumannite) = –49470 (±130) J/mol,
$S°(Ag_2Se$, low naumannite) = 149.99 (±0.56) J/(K·mol);
$\Delta_f G°(Ag_2Se$, high naumannite) = –47430 (±290) J/mol,
$S°(Ag_2Se$, high naumannite) = 169.01 (±0.78) J/(K·mol);
$\Delta_f G°(Ag_3AuSe_2$, fischesserite) = –86450 (±320) J/mol,
$S°(Ag_3AuSe_2$, fischesserite) = 290.80 (±1.26) J/(K·mol);
$\Delta_f G°$(β-AuSe) = –4110 (±1300) J/mol;
$S°$(β-AuSe) = 75.49 (±3.55) J/(K·mol).

The phase transition point for low naumannite-high naumannite was determined at T_{trs} = 405.4 K, with the enthalpy of transition of $\Delta_{trs}H$ = –7713 (±550) J/mol.

Keywords: Thermodynamic data, naumannite, fischesserite, AuSe, EMF-method, solid-state galvanic cell

Introduction

The class of selenides, and selenides of noble metals in particular (including system Ag-Au-Se), are rare but characteristic minerals of the Ag-Au-S-Se-Te hydrothermal deposits. The existence of low-temperature silver selenide—naumannite—has been known for a long time (Earley 1950). Fischesserite (Ag_3AuSe_2) was discovered (Johan et al. 1971) in the carbonate veins of Predborice, Bohemia, Czechoslovakia (now Czech Republic), where it was associated with naumannite, clausthalite (PbSe), berzelianite ($Cu_{2-x}Se$), gold, and other selenides. The phase AgAuSe was synthesized by Nekrasov et al. (1990). Gold selenide (AuSe) was never found in the nature. The only gold and silver selenide Ag_3AuSe_2 occurs in many gold-silver deposits, and its thermodynamic properties are very important in understanding geochemistry, transport, and deposition of gold.

The objectives of the present study are to explore the phase relations in the Ag-Au-Se system below the temperature of the α-β transition in Ag_2Se and to determine the standard thermodynamic properties of fischesserite, naumannite, and β-AuSe using electromotive force (EMF) measurements in solid-state galvanic cells. This method has proved to be direct, effective, and most accurate for determination of molar free energy and molar entropy change in reactions (Kiukkola and Wagner 1957a, 1957b).

Ag-Au-Se system and marginal systems. This ternary system Ag-Au-Se has not been studied experimentally. However, its marginal binary and pseudo-binary sections were studied quite intensely (Karakaya and Thompson 1990; Wiegers 1976; Rabenau et al. 1971; von Oehsen and Schmalzried 1981). The results of these works provide the relatively complete picture of low-temperature phase relations in the ternary system (Fig. 1a).

The system Ag-Se. The Ag-Se binary phase diagram was

* E-mail: euo@iem.ac.ru

reviewed by Karakaya and Thompson (1990). Ag_2Se(cr) is the only intermediary phase in the system and exists in two polymorphs, β and α. The β-polymorph (low naumannite) is stable below 406 K. The thermodynamic properties of silver selenide were recently reviewed by Olin et al. (2005).

The system Ag-Au. A complete miscibility between silver and gold is established for a wide range of temperatures. Ag-Au alloys are called electrum, and their thermodynamic properties are not used in this study.

The system Au-Se. The gold–selenium phase diagram was investigated by Rabenau et al. (1971). Two polymorphs, α and β (low temperature) with AuSe composition were found. The α-polymorph is subject to eutectoid decomposition at 698 K, and the β-polymorph is metastable. The authors pointed out that, although the β-polymorph is probably metastable, there is no direct evidence, and this problem is still open for further investigation. No other compounds are known in this system. Accordingly to Rabenau and Schultz (1976), the valence formula of both compounds can be written as $Au^+Au^{3+}(Se^{2-})_2$. In both modifications, Au^+ and Au^{3+} are coordinated by two and four selenium atoms, respectively, and each Se atom is bonded to one Au^+ and two Au^{3+} atoms.

The system $Ag_{2-x}Au_xSe$. According to Wiegers (1976), this system is pseudo-binary in the range of $0 < x < 0.5$. Two ordered compounds exist at temperatures below 406 K: β-Ag_2Se (naumannite) and β-Ag_3AuSe_2 (fischesserite). At higher temperatures, a solid solution with the α-Ag_2Se (high naumannite, body centered cubic) structure exists over the whole composition range (Fig. 1b).

The phase AgAuSe (x = 1) was synthesized by Nekrasov et al. (1990) from elements by the method of dry synthesis in evacuated quartz glass capsules. The synthesis temperature was 1023 K (for 4 days) with subsequent annealing at 573 K for one month. The X-ray diffraction pattern of the resulting compound was found to be identical to natural petrovskaite (AgAuS) (Nesterenko et al. 1984).

Experimental methods

99.95% and 99.99% gold and silver foil, 99.999% selenium, and gold powder (Aldrich Chem. Co.—20 mesh, 99.999+%) were used for synthesis of experimental phases.

To characterize the solid phases and to prepare electrodes (sample system), fischesserite and mixture of $Ag_3AuSe_2 + 2Ag_2Se$ were prepared in batches of 1–1.2 g by reacting Ag-Au alloys (electrum) and selenium. Several compositions of electrum were synthesized by fusing a mixture of small pieces of gold and silver in a silica glass ampoule in a hot oxy-gas flame. The alloy obtained was flattened to ~0.2 mm thick foil and cut into small pieces, ~0.5 × 2 mm in size. A weighed amount of electrum was then loaded together with a stoichiometric amount of selenium into a silica-glass tube. To eliminate most of the vapor phase, a tightly fitting silica glass rod was inserted into the tube, which was subsequently evacuated (to $\sim 10^{-4}$ atm) and sealed. The synthesis was performed in horizontal tube furnaces. For the first 3–4 days of synthesis, the charged tube was annealed at 673 K to allow the liquid selenium to react with electrum, after which it was heated to 873 K and annealed for other 1–2 days. Then the tube was cooled down by turning off the furnace (~14 hours to room temperature) and opened. The XRD analysis of the synthesized samples indicated pure phases or mixtures of desired compositions. To eliminate possible heterogeneities, the synthesized selenide material was ground, loaded again into a silica glass tube, and the same annealing procedure was repeated.

The binary compounds Ag_2Se (naumannite) and AuSe were prepared by direct synthesis from elements (gold powder). The annealing was performed at 573 K for two weeks with one intermediate grinding. AuSe was also synthesized in excess, approximately 10 mass% of gold powder for β-polymorph, according to the data of Rabenau et al. (1971).

The resulting products were examined by XRD (DRGP-4, AZG-4, 35 kV/30 mA). The powder patterns corresponded to JCPDS card 25-0367 for fischesserite (Johan et al. 1971), 24-1041 for low naumannite (Wiegers 1976), and 81-2227 for β-AuSe (Rabenau et al. 1971). The X-ray patterns of low naumannite, fischesserite, and β-AuSe are given in Tables 1, 2, and 3 respectively. Also, the lattice parameters of fishesserite and β-AuSe were calculated from obtained XRD-specters: low naumannite—a = 0.4350 (0.0003) nm, b = 0.7075 (0.0005) nm, c = 0.7769 (0.0004) nm; fischeserrite—a = 0.9961 (0.0002) nm; β-AuSe—a = 0.8363 (0.0004) nm, b = 0.3668 (0.0002) nm, c = 0.6266 (0.0004) nm, β = 106.01° (0.05). Lattice parameters calculated for β-AuSe coincide well with Rabenau et al.'s (1971) data. All parameters were calculated by using the information-calculating system on crystal structure data of minerals "MYNCRIST" (Chichagov et al. 1990).

All synthesized phases and phase mixtures were examined in a reflected light. The pure elements Au, Ag, Se, and synthesized naumannite, fischesserite, and β-AuSe phases didn't contain any extra phases and were used as microprobe standards (phases were used as standards after elements' analysis to take into account parameters of atom's cooperation). The analysis of cell sample systems after

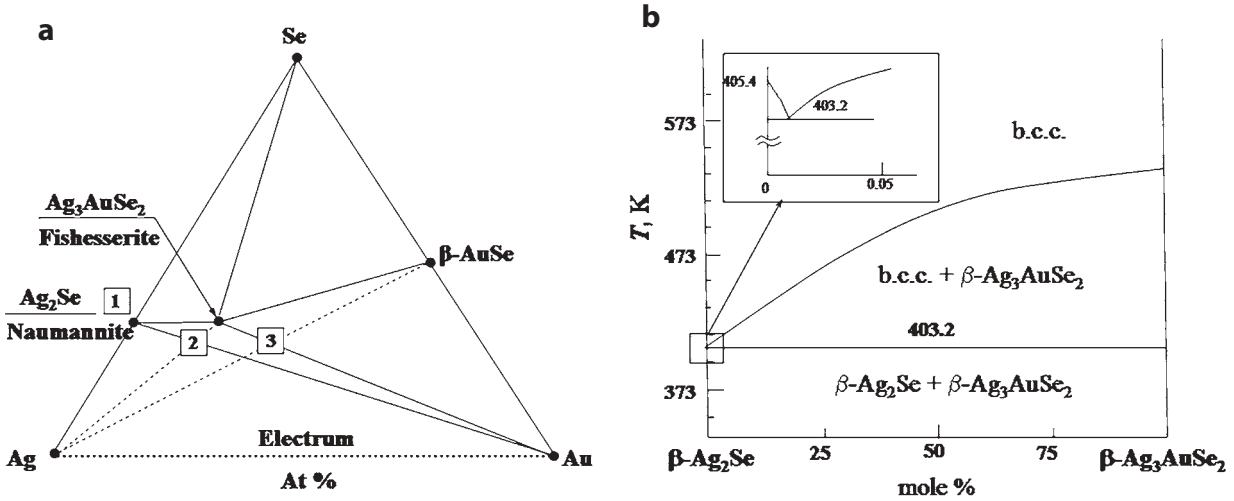

Figure 1. (**a**) Phase relations in the system Ag-Au-Se at 298–403 K and total Ar-gas pressure of 1 atm. The numbers of studied phase reactions 1, 2, and 3 are given in boxes. (**b**) Temperature-composition diagram for the pseudobinary system Ag_2Se-Ag_3AuSe_2 (after Wiegers 1976). The eutectoid position is shown in inset; b.c.c. denotes solid solution with body-centered cubic lattice.

TABLE 1. X-ray data for Ag_2Se

d (nm)	I (%)	*hkl*
28.95	23	102
26.83	100	112
25.90	80	121
24.36	46	013
22.60	48	031
21.26	39	113
20.97	29	201
20.16	33	032
18.73	28	014

Note: CoKα radiation, Fe-filter, 15–30 °θ, step 0.01 °θ, time of exposure 1 s.

TABLE 2. X-ray data for Ag_3AuSe_2

d (nm)	I (%)	*hkl*
70.54	30	110
31.52	19	310
28.72	21	222
26.63	100	321
23.51	19	411/330
22.28	29	420
20.35	29	422
19.54	17	$\bar{5}10$/431
18.20	21	521

Note: CoKα radiation, Fe-filter, 5–45 °θ, step 0.01 °θ, time of exposure 1 s.

TABLE 3. X-ray data for β-AuSe

d (nm)	I (%)	*hkl*
40.30	70	200
38.87	21	$\bar{2}01$
33.38	11	110
30.77	23	$\bar{1}11$
28.14	44	$\bar{2}02$
27.91	100	111
22.00	31	$\bar{3}11$
21.46	18	202
20.38	16	$\bar{2}03$
20.10	15	400
19.38	22	$\bar{4}02$
19.07	31	311
18.36	21	020
18.17	25	$\bar{1}13$
16.69	20	$\bar{3}13$
15.24	20	$\bar{5}11$
13.94	10	222

Note: CoKα radiation, Fe-filter, 7–35 °θ, step 0.01 °θ, time of exposure 1s.

experiments were made with fully PC-controlled Scanning Electron Microscope VEGA TS 5130MM (CamScan MV2300) equipped with BSEdetector and EDX microanalyzer (accelerating potential U = 20 kV). The compositions of fischesserite (in intergrowths with Au) and β-AuSe were determined as $Ag_{3.00}Au_{0.99}Se_{2.01}$ and $(Ag_xAu_{1-x})Se_{1.00}$, respectively, where $0.03 \le x \le 0.05$. The discrepancy from stoichiometric AuSe can be explained due to a formation of narrow range of solid solution.

The sample system for Cell A (Ag_2Se + Se, mole ratio 2:1) was prepared by direct synthesis from the mixture of silver and selenium. Selenides for the electrode (sample system) of Cell B were prepared by direct synthesis from the mixture (mole ratio 1:1) of selenium and electrum $Ag_{0.875}Au_{0.125}$. The sample system for this cell was prepared by grinding gold powder together with the selenide mixture (mole ratio Ag_2Se:Ag_3AuSe_2:Au was equal to 2:2:1). The sample system for Cell C was prepared from the mixtures of AuSe synthesized from elements with small excess of gold, Ag_3AuSe_2, and Au powder in the mole ratio of 2:2:1. The electrode tablets (2 mm in thickness and 6 mm in diameter, ~0.4 g mass) were pressed under 2 ton load, and then their flat surfaces were mirror-polished.

The silver electrodes (reference system) were prepared from silver rod 3–4 mm in thickness and 6 mm in diameter. The solid electrolyte tablet (2–3 mm thick and 5–6 mm in diameter) was cut from a block of crystalline transparent yellow-green Ag_4RbI_5, and its flat surfaces were mirror-polished. The cell in the form of a tablet stack was placed into a silica glass tube (6.5 mm ID) between Pt disks, which were connected with Au leads and adjusted by spring to improve the electrical contact (the responsibility of the electrical contact was checked by changing loading and vibration of the cells arrangement at the time of running). Finally, the cell holder was placed into another silica glass tube (11 mm ID) with gas inlet and outlet spouts. Measurements were performed under a dried argon gas flow of 0.5–1 cm^3 per minute.

All the experiments were carried out in vertical resistance furnaces, in which inner ceramic tubes had the dimensions of 18 mm ID × 240 mm height, and the diameter of the thermal insulations wall was 160 mm. The lower end of the furnace tube was closed with a ceramic stopper (with a hole 2–4 mm in diameter) to optimize the air convection. The isothermal zone (±0.1 K) was managed to establish within at least 20 mm in the central part of the furnace. The furnaces were powered by a DC source. Temperature in the furnace was controlled to at least ±0.15 K using a PROTERM 100 high-precision temperature controller. The regulating thermocouple (Pt/Pt, 10 mass% Rh) was placed in the immediate vicinity of the heating coil. Temperature and EMF were measured by a SCH304-2 multichannel digital millivoltmeter with accuracy of ±0.005 mV. The entrance channel resistance for EMF measurements was 10^{12}–10^{13} Ohm. The cell temperature was measured by a chromel-alumel thermocouple ("K" type). Galvanic cell design and cell operation were the same as described by Osadchii and Rappo (2004).

Below 405 K, fischesserite in equilibrium with naumannite is a strictly stoichiometric phase (Wiegers 1976). All attempts to obtain the AgAuSe phase in the temperature range 350–773 K were not successful. In the experiments at temperatures above 673 K, the quenched samples only contained the fischesserite, while at temperatures below 550 K, the assemblage of fischesserite with β-AuSe and Au became stable. The actual temperature of the solid-solution breakdown could not be determined by quenching technique due to the fast rate of the reaction.

The phase diagram only showing the stable phases of constant composition is given in Figure 1a. This diagram was used as a background for designing the phase reactions for EMF experiments and for determining the upper temperature limit for the reactions with fischesserite.

RESULTS AND DISCUSSIONS

Phase reactions and galvanic cells

The following reactions were studied to determine the thermodynamic properties of Ag_2Se, Ag_3AuSe_2, and AuSe:

$$2Ag(cr) + Se(s) = Ag_2Se(cr) \quad (1)$$
$$Ag(cr) + Ag_3AuSe_2(cr) = 2Ag_2Se(cr) + Au(cr) \quad (2)$$
$$3Ag(cr) + 2AuSe(s) = Ag_3AuSe_2(cr) + Au\ (cr) \quad (3)$$

These reactions were realized in the form of all solid-state galvanic cells with Ag_4RbI_5 superionic compound, which has a specific Ag^+ conduction (Despotuli et al. 1989), as a solid electrolyte:

A: (–) Pt | Ag | Ag_4RbI_5 | Se, Ag_2Se | Pt (+)
B: (–) Pt | Ag | Ag_4RbI_5 | Ag_3AuSe_2, Ag_2Se, Au | Pt (+)
C: (–) Pt | Ag | Ag_4RbI_5 | Ag_3AuSe_2, AuSe, Au | Pt (+)

The principle of determination of cell polarity and half-cell reactions is the same as that described by Osadchii and Rappo (2004) for the system Ag-Au-S.

Reactions 1–3 are consistent with the Ag-Au-Se phase diagram at temperature below 406 K (Fig. 1a). All selenides in this system are stable in the presence of pure gold or selenium, whereas pure silver and silver-rich electrum react with all phases except Ag_2Se. We also assume that the homogeneity range of naumannite, fischesserite, and β-AuSe is very narrow (Wiegers 1976). The upper temperature limit for studying Reactions 2 and 3, including the stoichiometric phase, is 406 K. For reaction 1, the upper temperature limit was estimated as the melting point of selenium (494 K). The lower temperature limit was chosen for each cell so that to enable stable and reproducible EMF readings.

EMF values

EMF measurements were carried out as "temperature titration," i.e. stepwise heating with waiting for a constant (equilibrium) EMF value at each given temperature. The following procedure was used to control the accuracy and reproducibility of the EMF data. Initially, the cell was slowly heated to a certain temperature, e.g. 373 K. After the equilibrium EMF was attained, the temperature was increased in 20 K steps to the maximum value and then decreased by 10 K and further down in 20 K steps to the minimum temperature. Then, temperature was increased again by 10 K and raised in 20 K steps back to 373 K. The second temperature titration loop started at 5 K higher (378 K) and the heating continued in 10 K steps. As a result, all data points taken were 5 K apart, and the adjacent points were separated one from another by a significant period of time. For additional precision control, EMF was measured repeatedly at some points (in 5, 10, or 20 K steps).

The control time of reaching the equilibrium EMF value at a given temperature ranged from 12 hours to 5–6 days. The EMF data acquisition was performed automatically in a non-stop regime with a frequency of 1 Hz, and every 5 min the three most recent measurements were averaged and saved in a computer file. The current results were plotted vs. time, and the graphic visualization helped to evaluate the approach to equilibrium. The last 20–40 data points (100–200 min interval) were averaged and saved in a data table, if the EMF values did not differ significantly from the data obtained during the previous hours. The equilibrium state was assumed when the EMF and temperature values stayed constant within ±0.02 mV and ±0.15 K, respectively, over a period of several hours to 1 day.

At all experimental conditions studied, the equilibrium was reached after no more than 48 hours. After the cell was short-circuited for 10–60 s and/or polarized at 1.018 V (Weston element) with direct and reverse polarity, the EMF returned to the equilibrium value within 6–24 hours over the whole temperature range. The replacement of Pt inert electrodes to graphite did not make changes in EMF values.

The EMF values (E) measured in Cells A–C as a function of temperature are listed in Table 4 (in temperature order) and shown in Figure 2. Fitting the linear equation $E = a + bT$, which implies that $\Delta_t C_p$ is constant and equal to zero, to these experimental data yielded the following equations:

$$E(\mathrm{A})/\mathrm{mV} = 221.43\ (\pm 0.68) + 0.1172\ (\pm 0.0019)\cdot T/\mathrm{K},\ (317 < T/\mathrm{K} < 406),\ \mathrm{R} = 0.999 \quad (4)$$

$$E(\mathrm{A})/\mathrm{mV} = 181.46\ (\pm 1.46) + 0.2158\ (\pm 0.0034)\cdot T/\mathrm{K},\ (398 < T/\mathrm{K} < 457),\ \mathrm{R} = 0.999 \quad (5)$$

$$E(\mathrm{B})/\mathrm{mV} = 85.51\ (\pm 1.94) + 0.147\ (\pm 0.005)\cdot T/\mathrm{K}\ (310 < T/\mathrm{K} < 402),\ \mathrm{R} = 0.994 \quad (6)$$

$$E(\mathrm{C})/\mathrm{mV} = 209.41\ (\pm 4.12) + 0.204\ (\pm 0.011)\cdot T/\mathrm{K}\ (320 < T/\mathrm{K} < 480),\ \mathrm{R} = 0.994 \quad (7)$$

The confidence interval 95% (±2δ) of the experimental data was calculated by the least-square method.

Table 4 and Figure 2 show also the high-temperature points

Table 4. Measured temperatures and EMF (E_{meas}) of galvanic Cells A–C, and values of $\Delta E = E_{meas} - E_{calc}$, where E_{calc} is calculated using Equations 4–7 and 9

T (K)	E_{meas}, (mV)	ΔE (mV)
Cell A, Reaction 1, Equation 4, Run K-3		
317.8	258.64	–0.04
320.3	258.93	–0.04
322.7	259.18	–0.07
325.1	259.62	0.09
327.6	259.79	–0.04
330.4	260.36	0.21
333.4	260.41	–0.10
336.3	261.03	0.18
339.1	261.11	–0.06
341.8	261.68	0.19
344.6	261.84	0.02
347.3	262.28	0.15
350.2	262.51	0.04
352.7	262.82	0.05
355.9	263.09	–0.05
358.1	263.40	0.00
361.2	263.67	–0.09
363.5	264.00	–0.03
366.4	264.27	–0.10
368.8	264.50	–0.15
371.8	264.88	–0.13
374.0	265.22	–0.04
377.0	265.42	–0.20
379.3	265.82	–0.06
382.2	266.01	–0.21
384.7	266.62	0.10
387.7	266.70	–0.17
390.4	267.32	0.13
393.8	267.38	–0.20
396.0	268.03	0.19
401.7	268.73	0.22
407.1	269.39	0.25
Cell A, Reaction 1, Equation 5, Run K-3		
399.0	267.80	0.23
399.3	267.70	0.07
404.5	268.78	0.03
404.6	268.91	0.14
407.4	269.37	–0.01
410.2	269.94	–0.04
410.2	270.06	0.08
412.6	270.54	0.04
415.4	271.05	–0.06
415.5	271.07	–0.06
418.1	271.63	–0.06
420.9	272.21	–0.08
423.3	272.85	0.04
426.1	273.31	–0.10
426.2	273.25	–0.19
429.8	274.12	–0.09
431.4	274.47	–0.09
433.8	274.97	–0.11
436.5	275.89	0.23
436.7	275.41	–0.29
436.8	275.69	–0.03
441.7	276.70	–0.08
444.2	276.97	–0.35
447.0	278.12	0.19
447.0	278.13	0.20
451.9	279.12	0.14
456.9	280.33	0.27
457.1	280.13	0.03
Cell B, Reaction 2, Equation 6, Run A-582		
316.1	132.76	0.74
321.4	132.90	0.09
325.7	133.95	0.51
325.9	133.90	0.43
326.0	133.26	–0.22
331.0	134.57	0.35
331.3	134.29	0.02
336.9	134.80	–0.30
337.0	135.42	0.32
342.2	135.14	–0.73
342.3	136.30	0.41

TABLE 4. —*Continued*

T (K)	E_{meas}, (mV)	ΔE (mV)	T (K)	E_{meas}, (mV)	ΔE (mV)
342.3	135.38	–0.51	339.6	278.07	–0.69
342.5	135.29	–0.63	342.4	278.80	–0.53
347.8	137.16	0.46	342.5	279.08	–0.27
347.9	136.60	–0.11	342.6	280.63	1.26
353.0	137.10	–0.37	348.0	280.16	–0.31
353.2	137.70	0.20	348.2	281.09	0.58
353.4	137.10	–0.43	353.2	281.32	–0.21
358.6	139.02	0.73	353.4	282.82	1.25
358.6	138.12	–0.18	358.7	282.59	–0.07
363.7	138.90	–0.15	358.8	283.58	0.90
364.0	139.56	0.47	363.9	284.94	1.22
364.2	138.94	–0.18	364.0	283.62	–0.12
369.0	139.60	–0.23	369.3	284.73	–0.09
369.2	140.16	0.31	369.4	285.82	0.98
374.2	140.20	–0.39	374.5	286.88	1.00
374.3	140.82	0.21	374.5	285.68	–0.20
374.5	140.30	–0.34	379.6	286.57	–0.35
379.2	141.50	0.17	379.7	287.69	0.75
379.4	141.31	–0.05	385.1	287.48	–0.57
379.5	141.48	0.11	385.2	288.58	0.51
384.7	141.60	–0.55	390.6	288.52	–0.65
384.9	142.27	0.10	390.8	289.60	0.39
385.2	142.60	0.39	396.0	289.83	–0.44
390.1	143.49	0.55	396.1	290.40	0.11
390.5	143.19	0.19	396.2	289.54	–0.77
395.7	143.00	–0.77	396.3	289.44	–0.89
396.1	144.10	0.28	401.7	291.31	–0.13
396.2	143.20	–0.64	unaccounted points		
396.3	143.90	0.05	406.9	292.11	0.71
401.1	145.18	0.62	407.0	291.96	0.54
401.1	144.00	–0.56	412.3	293.07	0.82
402.0	145.30	0.61	412.4	292.97	0.70
404.1	145.21	0.21	417.5	293.93	0.86
Cell B, Reaction 2, Equation 9, Run A-582			417.5	292.33	–0.74
404.1	145.21	–0.08	422.9	292.87	–1.06
406.7	146.64	0.08	427.8	295.61	0.91
407.2	147.18	0.38	427.8	293.73	–0.97
411.9	149.57	0.47	433.1	294.31	–1.23
417.9	151.45	–0.59	438.0	297.20	0.89
422.6	154.46	0.12	438.0	295.09	–1.22
427.8	156.42	–0.47	441.9	295.93	–1.00
433.0	159.39	–0.04	443.1	296.00	–1.12
438.0	161.57	–0.31	448.1	298.80	0.90
443.2	164.59	0.17	451.7	297.88	–0.59
448.1	166.75	–0.07	453.1	297.85	–0.84
453.1	169.67	0.40	458.7	300.36	0.78
Cell C, Reaction 3, Equation 7, Run A-619			462.5	300.51	0.33
325.8	274.99	–0.95	462.6	300.44	0.25
331.5	277.30	0.20	463.9	300.31	–0.09
336.8	277.05	–1.13	469.4	301.62	0.35
337.1	278.60	0.35	473.1	303.01	1.16
339.6	277.93	–0.83	483.7	304.51	0.98

that were not used for the calculation of thermodynamic functions because the phase compositions were not known. However, for the adopted starting bulk compositions, which do not change during the experiment, these data exhibit an excellent reproducibility. The distinct break in the Cell B data trend is related to the transition of the low naumannite to the solid solution with a body-centered cubic lattice and a composition strongly dependent on temperature (Fig. 1b). In Cell C, a reproducible hysteresis in the data trend in the range 412–470 K presumably results from the second-order transition in AuSe. The cross symbols in Figure 2 mark the data points obtained under decreasing temperature regime.

Calculations of thermodynamic properties

The Gibbs energy, entropy and enthalpy changes of the reaction can be calculated from the EMF values of galvanic cell using the base thermodynamic equations:

$$\Delta_r G = -nFE\cdot 10^{-3},$$
$$\Delta_r S = nF(dE/dT)\cdot 10^{-3},$$
$$\Delta_r H = -nF\cdot 10^{-3}\cdot[E - (dE/dT)T]$$

where n is the number of electrons participating in the overall cell reaction (2, 1, and 3 for the reactions 1, 2, and 3, respectively), F stands for the Faraday constant 96484.56 J/(mol·V), and E is the cell EMF in millivolts.

Standard thermodynamic properties of reactions 1–3 calculated using Equations 4, 5, 6, and 7 are listed in Table 5.

The temperature of the phase transition of low naumannite-high naumannite (or β-α, respectively) can be determined by joint solution of Equations 4 and 5. The enthalpy of transition can be found through the equation:

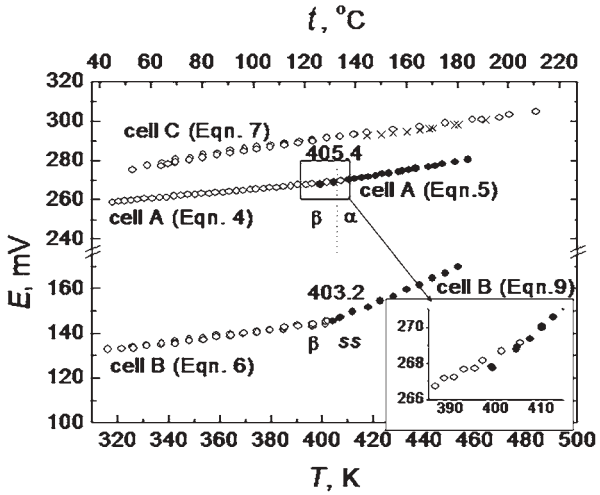

Figure 2. Temperature dependences of the EMF(E) of Cells A, B, and C. The reproducible over-cooling of Cell A is shown in inset; b.c.c. denotes $Ag_{2-x}Au_xSe_2$ solid solution. Cross symbols show the reproducible hysteresis and mark the data points obtained under decreasing temperature regime (see Table 3, unaccounted points).

$$\Delta_{trs}H(\beta\text{-}\alpha) = -n\mathrm{F}\cdot 10^{-3}\cdot\Delta[(\mathrm{d}E/\mathrm{d}T)]\cdot T_{trs} \quad (8)$$

The resulting values are T_{trs} = 405.4 K and $\Delta_{trs}H(\beta\text{-}\alpha)$ = –7713 J/mol.

It should be noted that overcooling was reproducibly observed in the experiment [Figs. 2 (insert) and 3, Table 4].

Temperature functions of the Gibbs energies of formation of the selenides from elements are also presented in the form of the equation $\Delta_fG_T = a + b\cdot T$ (Table 6).

The standard Gibbs energy of formation from elements and standard entropy of low naunannite, high naumannite, fischesserite, and β-AuSe at 298.15 K and 1 bar were calculated as follows:

$\Delta_fG°$(low naumannite) = $\Delta_rG°(1)$

$S°$(low naumannite) = $2S°$(Ag, cr) + $S°$(Se) + $\Delta_rS°(1)$

$\Delta_fG°$(high naumannite) = $\Delta_rG°(1)$

$S°$(high naumannite) = $2S°$(Ag, cr) + $S°$(Se) + $\Delta_rS°(1)$

$\Delta_fG°$(fischesserite) = $2\Delta_fG°(Ag_2Se, cr) - \Delta_rG°(2)$

$S°$(fischesserite) = $2S°(Ag_2Se, cr) + S°(Au) - S°(Ag, cr) - \Delta_rS°(2)$

$\Delta_fG°(\beta\text{-AuSe}) = 0.5[\Delta_fG°(Ag_3AuSe_2, s) - \Delta_rG°(3)]$

$S°(\beta\text{-AuSe}) = 0.5[S°(Ag_3AuSe_2, cr) + S°(Au) - 3S°(Ag, cr) - \Delta_rS°(3)]$

Standard thermodynamic properties of selenides in the Ag-Au-Se system at 298.15 K and 1 bar obtained in this study are compared to literature values in Table 7. This table also contains thermodynamic data for Ag(cr), Au(cr), and Se(cr).

Discussion

The all solid-state galvanic cell technique, which is used in this study, allows measuring the thermodynamic properties of the stoichiometric phases in a strict order: from naumannite to fischesserite to AuSe. The data for every next phase include the errors of the preceding estimates. Thus, with any other conditions being equal, the highest error can be expected for AuSe data, which contain errors of the values determined for Ag_2Se and Ag_3AuSe_2 as well as their own errors (Cell C). The data obtained for naumannite are the most accurate. The literature data reported by Kiukkola and Wagner (1957b), which were also obtained by EMF technique, are considered the most reliable (Olin et al. 2005). Gronvold et al. (2003) measured the heat capacity in the temperature range 298.15–900 K, and the Gibbs energy was determined by Mills (1974), who favored the galvanic cell studies by Kiukkola and Wagner (1957b). The EMF method was also used in the studies by von Oehsen and Schmalzried (1981) and Tokahashi and Yamomoto (1970).

Our results along with the data of the aforesaid authors are showing in Figure 3. This comparison demonstrates a good agreement of our values with those obtained by von Oehsen

Table 5. Thermodynamic properties at 298.15 K and 1 bar for reactions 1–3 calculated from experimental data listed in Table 3

Reaction/Equation	$\Delta_rG°$ (J/mol)	$\Delta_rH°$ (J/mol)	$\Delta_rS°$ [J/(K·mol)]
1/4	–49470 ± 130	–42730 ± 20	22.62 ± 0.37
1/5	–47430 ± 290	–35020 ± 90	41.64 ± 0.66
2/6	–12490 ± 180	–8280 ± 40	14.12 ± 0.48
3/7	–78240 ± 1210	–60610 ± 230	59.11 ± 3.24

Table 6. Coefficients a and b in equation $\Delta_fG_T = a + b\cdot T$

Phase	a (J/mol)	b [J/(K·mol)]	Temperature range (K)
low naumannite	–42729	–22.616	298.15–405.4
high naumannite	–35016	–41.643	405.4–457
fischesserite	–77174	–31.115	298.15–405.4
β-AuSe	–8280	13.996	298.15–405.4

Table 7. Standard molar thermodynamic properties for crystalline phases in the Ag-Au-Se system at 298.15 K and 1 bar

Phase	$\Delta_fG°$ (J/mol)	$\Delta_fH°$ (J/mol)	$S°$ [J/(K·mol)]	Source
Ag	0	0	42.55 ± 0.21	*
Au	0	0	47.49 ± 0.21	*
Se	0	0	42.27 ± 0.05	*
Ag_2Se (low naumannite)	–49472 ± 134	–42729 ± 286	149.99 ± 0.56	†
Ag_2Se (low naumannite)	–49020	–40620	155.54	‡
Ag_2Se (low naumannite)	–49410	–42360	151.03	§
Ag_2Se (low naumannite)	–46900 ± 1300	–40100 ± 1300	149.9 ± 0.5	||
Ag_2Se (high naumannite)	–47432 ± 292	–35016 ± 479	169.01 ± 0.78	†
Ag_2Se (high naumannite)	–50008	–40734	158.48	#
Ag_2Se (high naumannite)	–47520	–35000	169.38	‡
Ag_2Se (high naumannite)	–47484	–35050	169.09	§
Ag_3AuSe_2 (fishesserite)	–86451 ± 322	–77172 ± 611	290.80 ± 1.26	†
β-AuSe	–4107 ± 1296	–8361 ± 1832	75.49 ± 3.55	†
β-AuSe	–	–3766	86.61	**
α-AuSe	–	–7950	80.75	**

* Robie and Hemingway (1995).
† Present study.
‡ von Oehsen and Schmalzried (1981).
§ Gronvold et al. (2003).
|| Olin et al. (2005).
Kiukkola and Wagner (1957b).
** Rabenau et al. (1971).

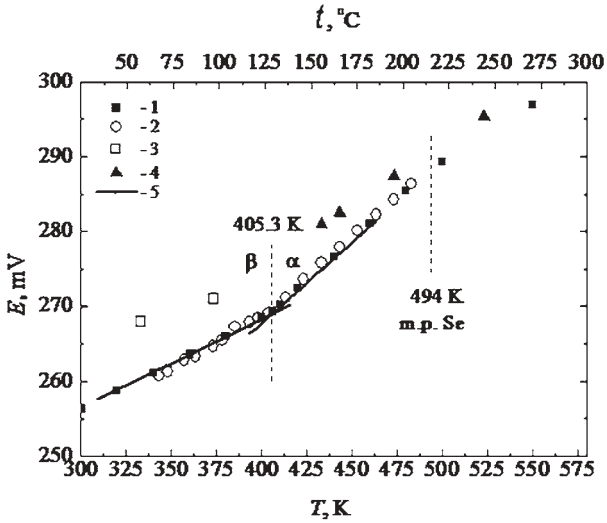

FIGURE 3. EMF (E) vs. temperature dependences for the reaction of naumannite formation from the elements according to different sources: 1 = Gronvold et al. (2003); 2 = von Oehsen and Shmalzried (1981); 3 = Takahashi and Yamamoto (1970); 4 = Kiukkola and Wagner (1957); 5 = this study.

and Schmalzried (1981) and a substantial discrepancy between our results and Tokahashi and Yamomoto's data (1970). As seen from Figure 3, Kiukkola and Wagner's (1957b) data significantly differ from other electrochemical measurements. It should be noted that these data were only obtained for high naumannite because AgI solid electrolyte, which was used in that work, only gains a notable ionic conductivity at temperatures above 420 K. Also, our results ideally coincide with the calorimetric data obtained by Gronvold et al. (2003). However, the reason for such a close agreement is not quite clear because the origin of approved value of $\Delta_f H_m(Ag_2Se, 298.15\ K) = -42650$ J/mol is not pointed to by the authors.

According to the electrical measurements by Wiegers (1976), the eutectoid temperature is equal (within experimental error) to the transformation temperature of Ag_2Se, and the eutectoid composition is probably close to the Ag_2Se composition (Fig. 1b). The data of Cell B (Table 4) that were not used in previous calculations can be treated to determine the eutectoid temperature and to estimate the enthalpy of the transition low naumannite into the $Ag_{2-x}Au_xSe$ solid solution with a b.c.c. structure. The experimental data of Cell B above the transition temperature are fitted to a linear equation:

$$E(\mathrm{B})/\mathrm{mV} = -52.25\ (\pm 1.60) + 0.4889\ (\pm 0.0124)\cdot T/\mathrm{K},\ (404 < T/\mathrm{K} < 453),\ R = 0.9992 \quad (9)$$

Solving together Equations 6 and 9, one can obtain the transition temperature, T_{trs}(β-b.c.c.) = 403.2 K. In the studied temperature range 403.2–453.1 K, the composition of the b.c.c. $Ag_{2-x}Au_xSe$ varies within $0 < x < 0.1$. The transition enthalpy, $\Delta_{trs}H_m$(β-b.c.c.) = –(6670 ±1000) J/mol, determined from Equation 8 is close to the enthalpy of the low naumannite-high naumannite transition. If Equation 6 is used and only the high-temperature data points closest to the eutectoid condition (Fig. 2) are taken into account, the transition enthalpy is estimated as $\Delta_{trs}H(\alpha\text{-ss}) = -(8100 \pm 1000)$ J/mol, while the transition temperature is the same. Such calculation seems to be most appropriate for a solid solution phase with composition strongly dependent on temperature. The eutectoid temperature is (3 ± 2) K lower than the transition temperature of Ag_2Se, which is consistent with the topology of a binary diagram with eutectoids. The eutectoid composition is unknown; however, based on Wiegers' data (1976), we can assume that it falls within $0.01 < x < 0.03$, and its effect on the enthalpy of the phase transition β-b.c.c. remains negligible within the experimental error. At high x values (up to the boundary with the b.c.c. single-phase field), the effect of the composition on the $E = f(T)$ dependence is within the experimental error.

Thermodynamic functions were first determined for fischesserite, and their accuracy can only be internally estimated. However, Cell B showed the most stable and reproducible EMF values within the whole temperature range studied.

Rabenau et al. (1971) measured the vapor pressure of $Se_2(g)$ in equilibrium with a mixture of gold and α- or β-AuSe in the temperature range from 505 to 602 K using the Knudsen effusion method. The molar enthalpy of formation and entropy at 298.15 K were calculated to $\Delta_f H_m^\circ$(AuSe, α, 298.15 K) = –7950 J/mol, S_m°(AuSe, α, 298.15 K) = 80.75 J/(K·mol) and $\Delta_f H_m^\circ$(AuSe, β, 298.15 K) = –3760 J/mol, S_m°(AuSe, β, 298.15 K) = 86.61 J/(K·mol), respectively. However, $Se_2(g)$ is not a major species in the gas phase at the temperature and total pressure used in that study. It was not stated how the partial pressure of $Se_2(g)$ was derived from the experimental data if only the total pressure was measured experimentally (Olin et al. 2005).

From our data (Table 7) the phase β-AuSe is thermodynamically stable and decomposes into elements ($\Delta_f G_m^\circ = 0$) at the temperature of (627 ± 10) K or above. Comparison of our thermodynamic properties of β-AuSe with the data obtained by Rabenau et al. (1971) suggests that they most probably dealt with the Rabenau's α-phase. According to X-ray data (Table 3), the sample system only contained the β-phase prior to the experiment. However, after the experiment, the α-phase was also found in the sample system in the amount of no higher than 10% of the β-phase content. Based on the results obtained and the available literature data, it is not possible to determine the relative thermodynamical stability of both polymorphs, and this issue remains open for further discussion.

The compound AuSe is of certain interest from geochemical point of view. For example, AuSe can be considered as a hypothetical end-member of solid solutions with sulfide minerals, such as arsenopyrite, pyrite, and pyrrhotite, which are typical members of many hydrothermal gold deposits.

ACKNOWLEDGMENTS

We are grateful to Ninell Lichkova (Institute of Microelectronics Technology and High Purity Materials, RAS, Chernogolovka) for synthesis of excellent solid electrolyte. We also thank A.V. Chichagov and Tatyana Dokina for XRD analysis of synthesized powders, Aleksey Nekrasov for microprobe investigations, and Mark Fedkin (Pennsylvania State University) for critical discussion and translation of the manuscript into English. Financial support was provided through RFBR grants No. 03-05-64380 and 06-05-64444.

REFERENCES CITED

Chichagov, A.V., Belonozhko, A.B., Lopatin, A.L., Dokina, T.N., Samohvalova, O.L., Ushakovskaya, T.V., and Shilova, Z.V. (1990) Information-Calculating System on Crystal Structure Data of Minerals (MYNCRIST). Cristallographija,

35, 3, 610–616 (in Russian); http://database.iem.ac.ru/mincryst/.

Despotuli, A.L., Zagorodnev, V.N., Lichkova, N.V., and Minenkova, N.A. (1989) New high conductivity solid state electrolytes: $CsAg_4Br_{3-x}I_{2+x}$ ($0.25 < x < 1$). Solid State Physics, 31, 9, 242–244.

Earley, J.W. (1950) Description and synthesis of the selenide minerals. American Mineralogist, 35, 337–364.

Gronvold, F., Stolen, S., and Semenov, Yu. (2003) Heat capacity and thermodynamic properties of silver (I) selenide, oP-Ag_2Se from 300 to 406 K and cI-Ag_2Se from 406 to 900 K: transitional behavior and formation properties. Thermochimica Acta, 399, 213–224.

Johan, Z., Picot, P., Pierrot, R., and Kvacek, M. (1971) La fischesserite, Ag_3AuSe_2, premier seleniure d'or, isotype de la petzite. Bulletin de la Society Francaise de Mineralogie et de Cristallographie, 94, 381–384.

Karakaya, I. and Thompson, W.T. (1990) The Ag-Se (silver-selenium) system. Bulletin of Alloy Phase Diagrams, 11, 266–271.

Kiukkola, K. and Wagner, C. (1957a) Galvanic cells for the determination of the standard molar free energy of formation of metal halides, oxides, and sulfides at elevated temperatures. Journal of the Electrochemical Society, 104, 308–316.

——— (1957b) Measurements on galvanic cells involving solid electrolytes. Journal of the Electrochemical Society, 104, 379–386.

Mills, K.S. (1974) Thermodynamic Data for Inorganic Sulphides, Selenides and Tellurides. Butterworths, London.

Nekrasov, I.Ya., Lunin, S.E., and Egorova, L.N. (1990) X-ray investigation of compounds of the system Ag-Au-S-Se. Dokladi Akademii Nauk USSR, 311, 4, 943–946 (in Russian).

Nesterenko, G.V., Kuznetsova, A.I., Pal'chik, N.A., and Lavrent'ev, Yu.G. (1984) Petrrovskaite AuAg(S,Se)—new selenium containing sulphide of gold and silver. Zapiski Vsesoyusnogo Mineralogicheskogo Obshestva, Part CXII, 5, 602–607.

Olin, A., Nolang, B., Ohman, L-O., Osadchii, E.G., and Rosen, E. (2005) Chemical thermodynamics of Selenium. In Nuclear Energy Agency Data Bank, Organisation for Economic Co-operation and Development, Ed., 7, 851 p. Chemical Thermodynamics, North Holland Elsevier Science Publishers B.V., Amsterdam.

Osadchii, E.G. and Rappo, O.A. (2004) Determination of standard thermodynamic properties of sulfides in the Ag-Au-S system by means of a solid-state galvanic cell. American Mineralogist, 89, 1405–1410.

Rabenau, A. and Schulz, H. (1976) The crystal structures of α-AuSe and β-AuSe. Journal of the Less-Common Metals, 48, 89–101.

Rabenau, A., Rau, H., and Rosenstein, G. (1971) Phase relations in the gold-selenium system. J. Less-Common Metals, 24, 291–299.

Robie, R.A. and Hemingway, B.S. (1995) Thermodynamic properties of minerals and related substances at 298.15 K and 1 bar (10^5 Pascals) pressure and at high temperatures. U.S. Geological Survey Bulletin, 2131.

Takahashi, T. and Yamamoto, O. (1970) Solid Ionics—Solid Electrolyte cells. Journal of the Electrochemical Society, 117, 1, 1–5.

von Oehsen, U. and Schmalzried, H. (1981) Thermodynamic Investigation of Ag_2Se. Berichte der Bunsen-Gesellschaft fur Physikalische Chemie, 85, 7–14.

Wiegers, G.A. (1976) Electronic and ionic conduction of solid solutions $Ag_{2-x}Au_xSe$ ($0 \le x \le 0.5$). Journal of Less-Common Metals, 48, 269–283.

MANUSCRIPT RECEIVED JANUARY 8, 2006
MANUSCRIPT ACCEPTED NOVEMBER 16, 2006
MANUSCRIPT HANDLED BY HONGWU XU